

# APPLICATION OF FINITE ELEMENT METHOD TO THE STRESS ANALYSIS OF HYDRO-TURBINE COMPONENTS

Takashi Kubota

Seiji Takimoto

Yoshiyuki Niikura

Kawasaki Factory

## I. INTRODUCTION

The finite element method (hereafter abbreviated as FEM) has been used as a computer code for stress analysis for twenty years. During this time, there has been a remarkable development of computer techniques and application theories related to the FEM code in accordance with the development of high speed, large capacity digital computers. Technical progress has included the development of various new elements, the large scale sparse matrix analysis method, the automatic generation of input data and the graphic display of output data. At present, economic, highly reliable and convenient FEM codes are widely used.

As its name implies, the FEM must simulate the object to be analyzed with appropriate finite elements (the so-called idealization or discretization into mesh). The analysis results may differ in accordance with the way of selection of the elements, the mesh sparseness, the method of providing suitable boundary conditions and the selection of load conditions. Therefore, unless the utility techniques above mentioned are established for the FEM code, its advantages will be lost no matter what excellent FEM codes are developed. This means that the development of excellent FEM codes and the establishment of utility techniques are inseparable and both are essential for the correct execution of the stress analysis.

These utility techniques are established only by verification of computed results of FEM code in comparison with strength tests of the structure to be analyzed. In the establishment of FEM utility techniques for the stress analysis of turbine components, the hydraulic development engineer must mediate between a software engineer and a construction designer.

Recently, there has been a tendency for hydro-turbines and pump-turbines to increase in capacity, size, head and speed. As hydro-turbines increase in size, the extent of deformation of the turbine component becomes important and it becomes necessary to investigate the deformation of the turbine components at the time of structural design. As the heads and speeds increase, the stress to which the


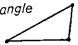
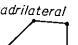
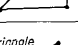
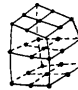

parts are subjected becomes very severe and calculating accurately the stress, and in particular understanding the positions and the values of stress concentration becomes indispensable in highly reliable structural design. As the heads and speeds increase, the stay vanes, wicket gates and runner vanes become thicker and the influence on their hydraulic performance can not be overlooked. In particular, the distribution of the stress on the complex three dimensional vane shapes such as runners can not be determined by the classical methods used in the past.

For the above reasons, stress analysis by the FEM in recent years has become very widespread in the structural design of turbine components as well as in the preceding projections. This article will give an explanation of the features of the FEM codes used by Fuji Electric and examples of the utility techniques for the various turbine components.

## II. FEATURES OF THE FINITE ELEMENT METHOD PROGRAM

In sections below, many examples are given and a comparison is made between FEM computation

Table 1 Element Types Used for Computation

Feature Type	Element shape	No. of nodal points	Degree of freedom of one nodal point	Displacement function
Axisymmetric and plane element	Quadrilateral 	4	$u, v$	Quadratic (Linear on boundary surface)
	Triangle 	3	$u, v$	Linear
Three dimensional shell element	Quadrilateral 	4	$u, v, w$ $\theta_x, \theta_y$	Deformation in plane: quadratic (linear on boundary surface) Bending deformation: cubic
	Triangle 	3	$u, v, w$ $\theta_x, \theta_y$	Deformation in plane: linear Bending deformation: cubic
Three dimensional solid element	Hexahedron 	27	$u, v, w$	Incomplete quadratic
	Pentahedron 	18	$u, v, w$	Incomplete cubic

and experimental results of strength tests. These computations are performed using various FEM codes including axisymmetric, plane, three dimensional shell and three dimensional solid elements as shown in *Table 1*.

In the FEM, there are the displacement method and the force method, but in these programs, the displacement method is always used. The following is a brief explanation of the features of the programs and elements used.

### 1. Axisymmetric and Plane Stress Analysis Programs

In the case of hydro-turbine components, there are many cases of shape idealization using two dimensional axisymmetric and plane elements in consideration of the easy input preparation and reduction of computing time. These programs are used frequently. There are two element shapes employed: the quadrilateral and the triangle. In the case of quadrilateral element, second order displacement function with its excellent similarity to the displacement field is used and in the case of triangular element, first order displacement function is used. It is also possible to use a mixture of both types of elements but it is better to use the more accurate quadrilateral elements except in cases when the use of the triangular elements can not be avoided because of the shape similarity relations.

Therefore, this program can perform very accurate and economical calculations with a little element discretization because of the use of the second order displacement functions. The degrees of freedom of the elements increase when higher order displacement functions are used, but in this program, the external freedom is eliminated at the stage of the formation of the stiffness matrix, so the numbers of simultaneous equations do not increase.

According to the computation results for the turbine head cover as an example of a comparative calculation between triangular elements of constant strain and quadrilateral elements of linear strain, results closer to the measured values are obtained with the quadrilateral element even though the element discretization of the elements is only 1/3 as rough as triangular elements.

The loads dealt with are concentrated load, distributed load (pressure), thermal load, centrifugal load, inertia force (gravity) and enforced displacement. The method of solving the simultaneous equations is the Gauss's method, but the computation time is shortened by using the band matrix properties and accurate results can be obtained.

### 2. Three Dimensional Shell Stress Analysis Program

Many of the turbine parts are welded structures using steel plates and these are best stress analysed as three dimensional structures of thin plates (three dimensional shell).

By combining these three dimensional shell ele-

ments, curved shape such as toroidal shells can also be handled. The element shapes are quadrilateral and triangular and as in the case of the axisymmetric program, the former is linear strain and the latter is constant strain for in-plane deformation<sup>(1)</sup>. For bending deformation, third order conforming displacement functions are used for both<sup>(2)</sup>. By combining the degrees of freedom of the in-plane and bending deformations, a three dimensional shell element is formed.

The loads handled are concentrated load, pressure load and enforced displacement. The simultaneous equations are solved by the Cholesky's method which is excellent for solving medium sized simultaneous equations.

The problem of pure bending of plates can be solved using this program.

### 3. Three Dimensional Solid Stress Analysis Program

The stress analysis of three dimensional curved shapes such as the wicket gate is to be performed by using the three dimensional curved elements shown in *Table 1*. In the case of three dimensional solid elements, however, there is a problem of the prolongation of the computation time because of the large number of degrees of freedom. These three dimensional curved elements are elements proposed by Argyris<sup>(3)</sup> and are hexahedron curved element with 27 nodal points and pentahedron curved element with 18 nodal points. Mixtures of both types of elements can be used together.

### 4. Input/Output

Generally, in FEM computations, there is a problem of a large amount of input/output data. However, by making a program using the methods shown later, the computation can be handled easily by an ordinary structural engineer.

For the input data, input check can be made merely by looking at an input figure by an X-Y plotter. Input preparation can also be simplified by automatic input data generation function. A large amount of output data processing can also be automated by making deformation and stress figures with an X-Y plotter. The following explains how to view some examples of output figures.

The stress figure shows the magnitude and direction of the stress at the centers of gravity of each element. In the stress figures of the axisymmetric program, the  $\bigcirc$  symbols indicate the tensile hoop stress and the  $\odot$  symbols the compression hoop stress. The magnitude of the stress is indicated by the diameters of these circles. The principal tensile stress in the plane is shown by the  $\leftrightarrow$  symbol and the principal compressive stress by  $\rangle\langle$ . The magnitudes of these stresses are indicated by the length of the arrows. The direction of the principal stress is shown by the arrow directions.

The stresses measured by experiments are shown

by the symbols  $\oplus$  and  $\triangle$ . These are connected by broken lines. The symbols for the hoop stress is  $\sigma_\theta$ , for the radial stress  $\sigma_r$  and for the principal stress  $\sigma_1$ .

The deformation figure shows the shape before deformation by broken lines and the shape after deformation by solid lines. The magnitude of the deformation is indicated by the deformation scale given in the figure. The arrows on the boundaries show the exterior forces exerted. The results of deformation measured by experiments are shown in the figure by the symbol  $\oplus$ .

### 5. Program Utility Techniques

The stress analysis of the hydro-turbine components is performed by using the various programs explained above. However, there are many cases where experience such as the method for determining the load and boundary conditions, the method for element discretization, etc. is utilized in the idealization of the problems to be analyzed. Therefore, a high level of program utility techniques are required for a complete FEM analysis.

In Fuji Electric, a considerable amount of experience has been obtained for the most suitable idealization of problems on the basis of large amount of experimental data. Program utility techniques are being developed so that reliable results can always be obtained.

## III. STRESS ANALYSIS OF INLET VALVE

### 1. Inlet Valve Case

The rotary type inlet valve case was formerly made of cast steel but it can now be made of a highly reliable welded structure because of the developments in welding techniques and recently, such structures are widely used. In the inlet valve cases (inlet diameter: 1,600 mm) of high head Francis turbine ( $H=410$  m,  $P=89$  MW), the stress was measured by strain gauges placed in locations where it was assumed that there will be stress concentration and the deformation was measured by dial gauges during the pressure withstand test (pressure:  $77\text{ kg/cm}^2$ ). Fig. 1 shows a photograph of a factory test.

In the stress analysis of the inlet valve case, the axisymmetric program is used because of the structural shape. Figs. 2 (a) and (b) show the

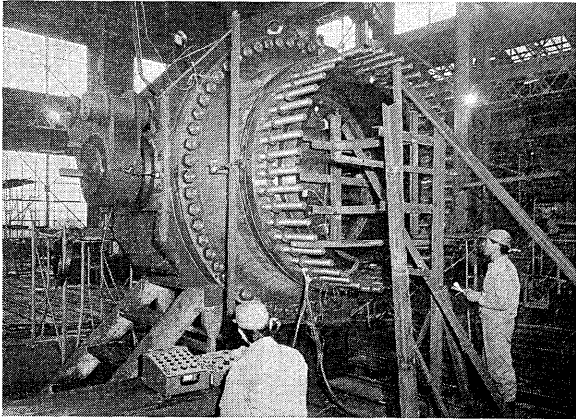
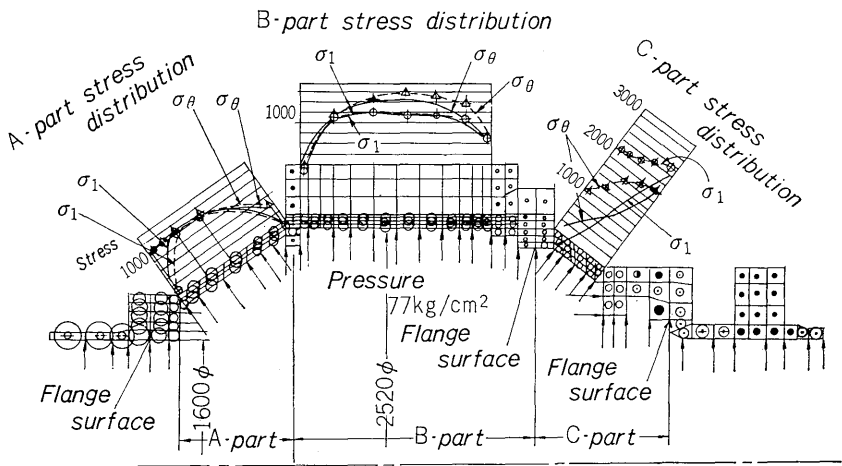
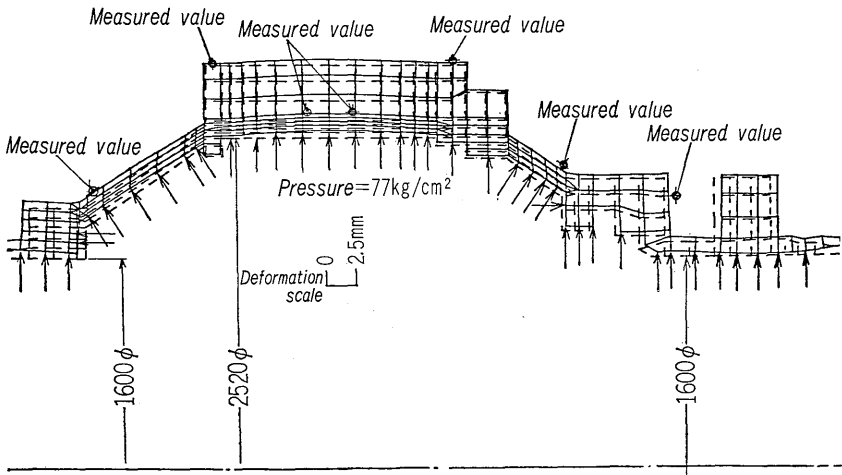


Fig. 1 View on stress test of inlet valve case

stress and deformation figures respectively comparing the computed and measured results. In the stress figure, the measured values of the hoop stress are shown by the symbol  $\triangle$  and the measured values of the principal stress by the symbol  $\oplus$ . The computed stress distribution in the A part agrees



(a) Stress figure



(b) Deformation figure

Fig. 2 Inlet valve case of high head Francis turbine ( $H=410$  m,  $P=89$  MW)

very well with the measured values. Because of the existence of the radial reinforced rib in the B part, there is some distortion in the hoop stress distribution by the axisymmetric FEM but there is good agreement for the principal stress distribution against the measured values.

There is some distortion between the computed stress distribution and the measured values in the C part for both the hoop and principal stresses. This is since the deformation is different in practice because of the excess stiffness by one body idealization even though the C part is a bolt joint structure on both ends. The measured values of the stress are rather high, but when they are converted to the maximum static pressure at site operation, they are less than 1/2 the yield points and present no practical problem.

The difference between the computed and measured values of the stress distribution for each part is evident from the deformation figure. The computed and measured values agree very well in A and B parts but the measured deformation in the C part is greater than the computed model because of the excess stiffness.

There are large number of bolt joint structures in the hydro-turbine components and when such structures are analyzed by the FEM, the handling of such joints and their idealization presents a very difficult problem. Stiffness reduction in the bolt joint part and problem of contact at flange parts are important themes which must be solved in the future.

## 2. Inlet Valve Disc

In the structural analysis of the inlet valve disc, three dimensional solid or shell program should be used because of its shape. However, considerable work is required to prepare the input data and computation takes a long time. Therefore, an example is shown here where the inlet valve disc was treated as a plane problem.

For the inlet valve disc (inlet diameter : 930 mm) of the high head Francis turbine ( $H=339$  m,  $P=33$  MW) shown in Fig. 3, the condition is most severe when completely closed at the maximum head,

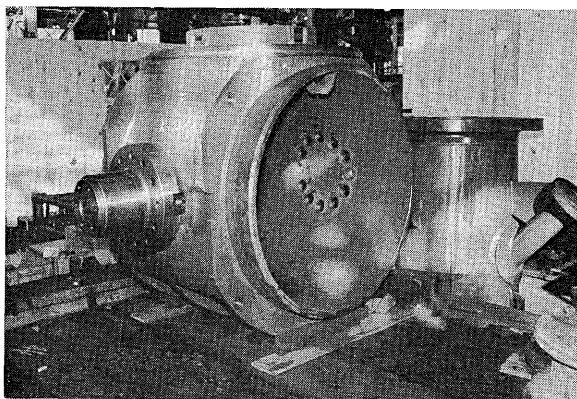


Fig. 3 View of inlet valve disc of high head Francis turbine

so the computation was executed for such a condition. The stress and deformation figures are shown in Figs. 4 (a) and (b) respectively.

There is a stress concentration at the root of the inlet valve shaft but its value is about  $1,000 \text{ kg/cm}^2$  and since the deformation was only  $0.25 \text{ mm}$  even in the sealing part, such a structure was found to present no problem in practice.

The inlet valve disc which at first glance would appear to be able to be treated only by three dimensional program could also be analyzed by plane stress analysis program. Therefore FEM can be used simply by both projection designers and line structural engineers so that components can be designed with a greater reliability than in the past.

## IV. STRESS ANALYSIS OF SPIRAL CASE AND STAY RING

### 1. Model Stay Ring of Conventional Turbine

Using the former construction, the model spiral

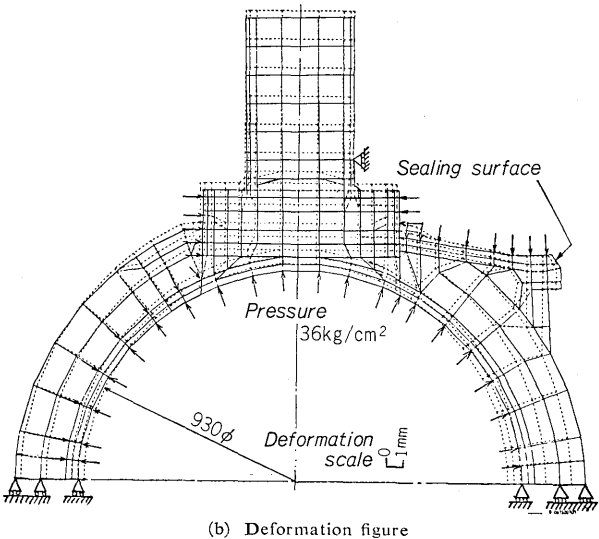
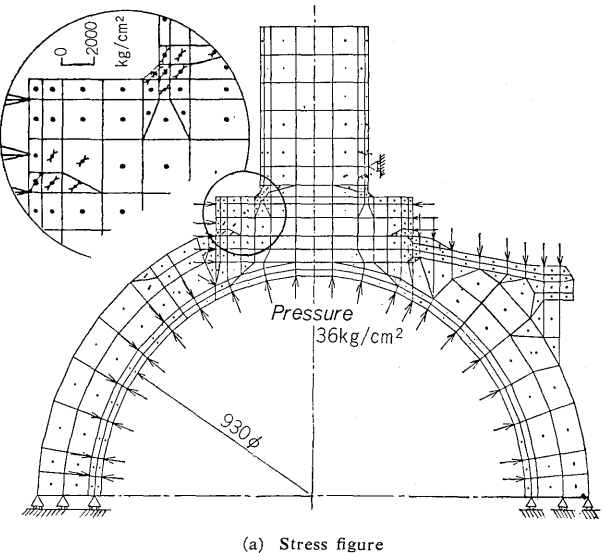


Fig. 4 Inlet valve disc of high head Francis turbine ( $H=339$  m,  $P=33$  MW)

case and stay ring of the Francis turbine ( $H=149\text{ m}$ ,  $P=22\text{ MW}$ ) with more than 10 years operating experience were manufactured and the stress and deformation were measured. A comparison with the results computed by FEM is shown in Fig. 5.

The stay vane was made of equally spaced 10 plates of 12 mm in thickness. When there are few stay vane plates, the crown plate stress is generally not distributed uniform in the hoop direction. However, even when the stress analysis is performed by axisymmetric program, the stress and deformation in the meridional plane of the assembly of spiral case and stay ring can be considered as simulated. In this case the calculation model is formed by converting the stay vanes into an axisymmetric material with equivalent stiffness to that of the actual stay vanes.

The analysis results using this technique are shown in Fig 5. The computed results of the case stress agree well with the measured values shown in parentheses. The computed results of the stress distribution in the leading and trailing edge of the stay vane are shown by the solid lines and the measured results by the broken lines and there is good agreement between the two. Therefore the propriety of the idealization formed by converting the stay vanes into an equivalent axisymmetric material was confirmed. Since it is evident that accurate calculations can be obtained even for a few numbers of stay vane, it has been confirmed that this technique can also be used without any problems for a large

number of stay vane such as in pump-turbine. The chain line with a dot in the figure on transition plate shows the result obtained by an approximate method (NEMA's method)<sup>(4)</sup> for stress analysis of the spiral case. The same type of line also shows the result obtained by using the Pamakian's method<sup>(5)</sup> for the stress on outer edge of the stay vane. Both of these methods show values which are average against the actual stress distribution, and no stress concentration is considered.

This turbine has been in operation for over ten years and there have been no particular problems during this time although the local stress concentration appears rather high because of the old type of construction. It is evident that such stress concentration can be traced sufficiently by FEM. This stress concentration occur because the force exerted on the scroll plate of the spiral case directly pull the tip of the stay vane, and this can be clearly understood from the deformation figure.

In order to avoid such stress concentration, the design should be such that the torsional moment around the center of gravity of the stay ring caused by the force exerted on the case decreases. The following is an example of a type newly designed considering this point.

## 2. Spiral Case and Head Cover of Large Francis Turbine

Fig. 6 shows a photograph of stay ring of the large capacity Francis turbine ( $H=165\text{ m}$ ,  $P=$

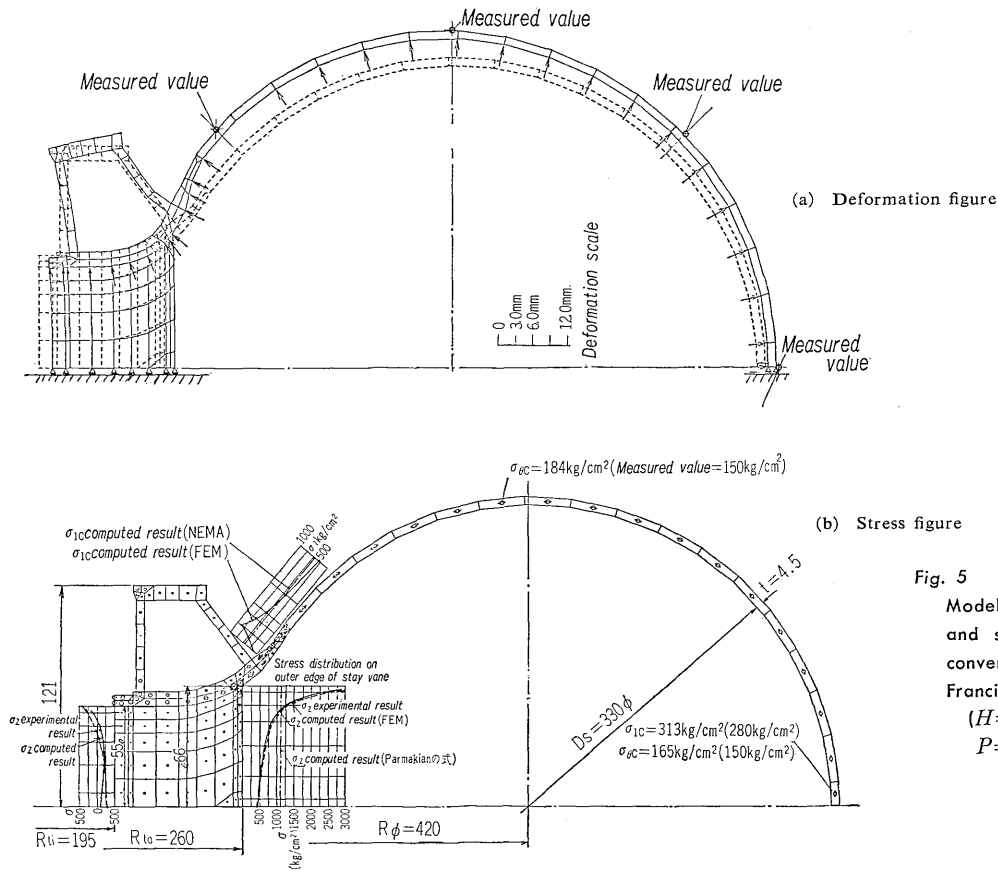


Fig. 5  
Model spiral case  
and stay ring of  
conventional  
Francis turbine  
( $H=149\text{ m}$ ,  
 $P=22\text{ MW}$ )

306 MW) which is analyzed. Figs. 7 (a) and (b) show the stress and deformation figure respectively at full load operation.

In order to eliminate the torsional moment around the center of gravity of the stay ring, the spiral case was welded directly to the central part of the stay vane. With such a structure, not only are stress concentration in the stay vane avoided, but the flow into the stay vane also becomes uniform by means of the attachment of the bell mouth ring as shown in Fig. 7 and the efficiency is better than the normal type. According to the analysis results, the stress values

and the flange parts of the head cover and stay ring. However, all stress values are less than 1/3 of the yield point and it was confirmed that this construction is satisfactory.

In the design of such high head pump-turbines, it is necessary not only to raise the head cover height and increase the whole stiffness, but also to increase the stiffness of the flange parts and keep the height up to the flange parts as low as possible in order to lower the stress and deformation values.

### V. HEAD COVER STRESS ANALYSIS

#### 1. Head Cover of Pump-Turbine

A model head cover, 1/5 scale of the prototype high head pump-turbine ( $H=377\text{ m}$ ,  $P=166\text{ MW}$ ) was manufactured and the stress and deformation was measured. Fig. 9 is a photo of the experimental equipment, but this model has no outer cylindrical rib because of the attachment of the strain gauges.

When the structural analysis was performed by FEM, the stress and deformation of the entire head cover were obtained by the axisymmetric program.

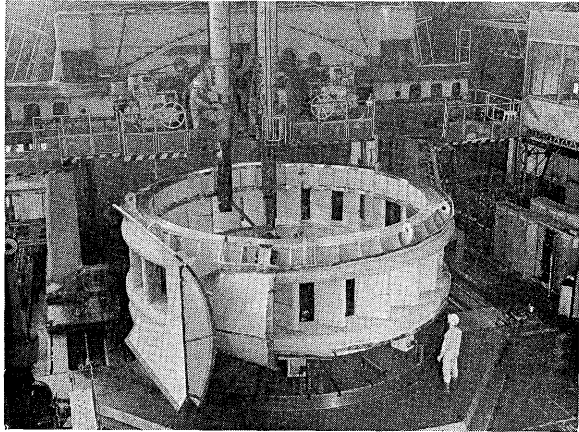


Fig. 6 View of stay ring of large Francis turbine

are higher in the transition plate than the stay vane inlet and there are no stress concentrations in the stay vane.

It is also necessary to investigate deformation in such large capacity turbines. The places which present major problems are the inside of the head cover and the bearing part of the wicket gate. As can be seen from the deformation figure in Fig. 7 (b) the deformation in the axial direction inside the head cover is only 1.03 mm. The inclination in the wicket gate bearing is also small and there is no need to worry about one side contact of the shaft.

#### 3. Case and Head Cover of High Head Pump-Turbine

An assembly of the case and head cover of a high head pump-turbine ( $H=530\text{ m}$ ,  $P=210\text{ MW}$ ) was analyzed. Fig. 8 shows the stress figure for the computed results during pump shut-off head operation. The large stress occurs in the transition plate

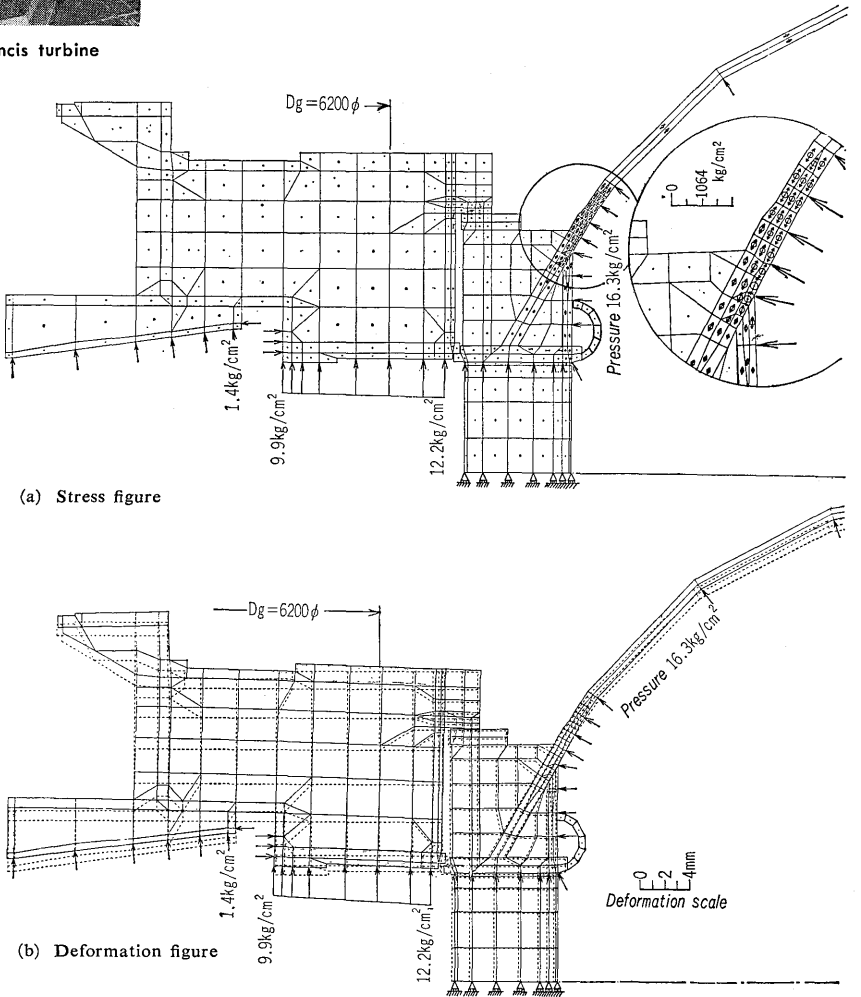


Fig. 7 Assembly of spiral case, stay ring and head cover of large Francis turbine ( $H=165\text{ m}$ ,  $P=306\text{ MW}$ )

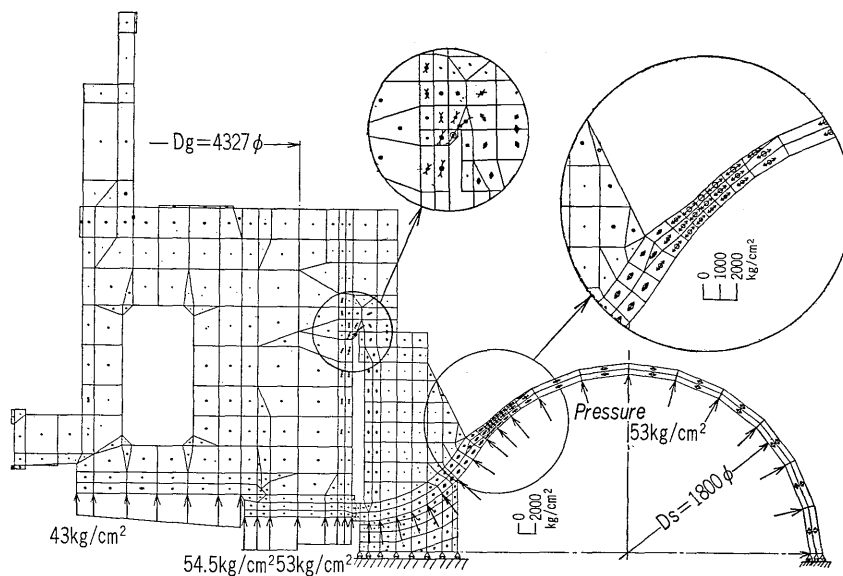


Fig. 8  
Stress figure of spiral case, stay ring and head cover assembly of high head pump-turbine ( $H=530$  m,  $P=210$  MW)

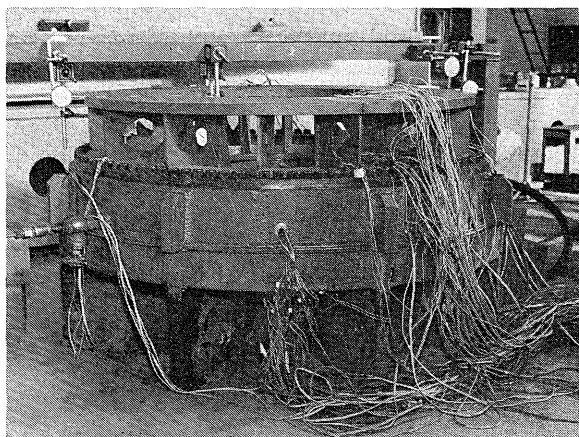


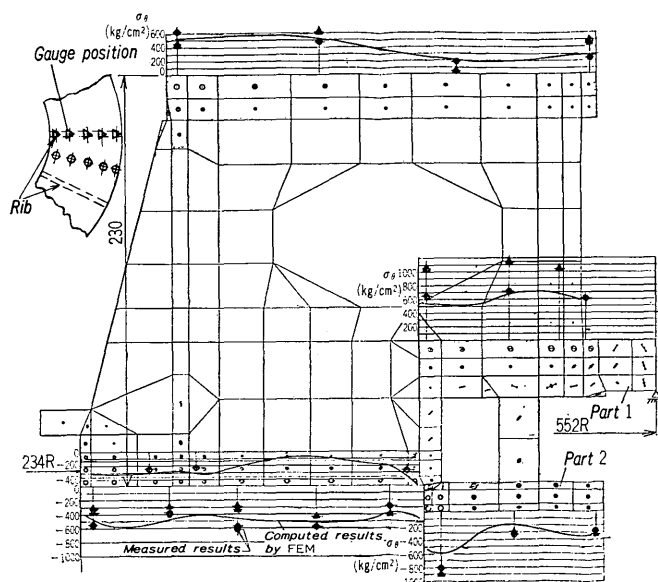
Fig. 9 View of stress test of model head cover

Then for the radial rib part, the computed deformation values were used as the given deformation and analysis was performed by the plane program.

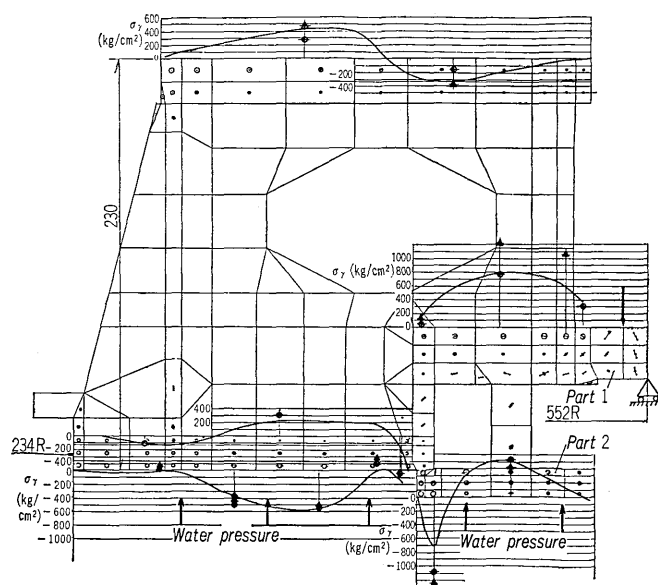
Fig. 10 shows the stress figure obtained by the axisymmetric program. The  $\oplus$  symbols in the figure show the stress values measured between the radial ribs and the  $\triangle$  symbols show the stress at the rib attachment parts. The FEM computation results are shown by the solid lines. Except for Part 1 including flange, there are no major differences between the  $\oplus$  and  $\triangle$  stress values, so the influence by the radial ribs is little. There is also good agreement with the computed results. This is because both the upper and lower plates are surrounded by radial and cylindrical ribs and there is little change in the stiffness in the circumferential direction.

Because there is no cylindrical rib on the outermost periphery in Part 1, the computed results by the axisymmetric program agree well with the measured results of the stress in the center parts between the radial ribs.

Fig. 11 shows a comparison of the computed and the measured results of the radial rib stress distribution. As was mentioned previously, the given deformation values obtained from the axisymmetric program were used as the input values in the com-



(a) Hoop stress



(b) Radial stress

Fig. 10 Stress figure of head cover ( $H=377$  m,  $P=166$  MW)



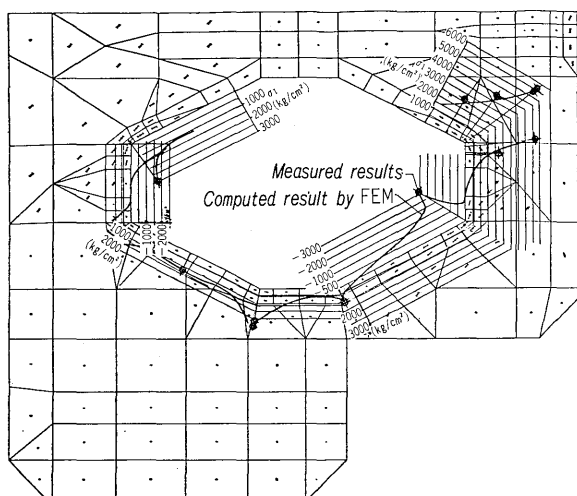


Fig. 11 Stress figure of radial rib of head cover

putation. In this method also, there was good agreement with measured values and the stress concentrations arising at the corner of the cutting window of the rib could be sufficiently analyzed.

For this high head pump-turbine presently under operation, measurements at site were made of deformations at turbine load rejection. The maximum deformation occurred when water pressure in the spiral case was a maximum. Fig. 12 shows the deformation figure of the results obtained by axisymmetric FEM when the maximum water pressure was applied to the head cover. There is good agreement between the computed and the measured results. This indicates that the deformation can be estimated with sufficient accuracy by the FEM not only for model test but also for site operation.

Fig. 13 shows the input figure when shell program was used. As can be seen from the figure, the analysis was performed for a cyclic segment with a rib.

## 2. Head Cover of Large Kaplan Turbine

Fig. 15 shows the deformation figure of the head

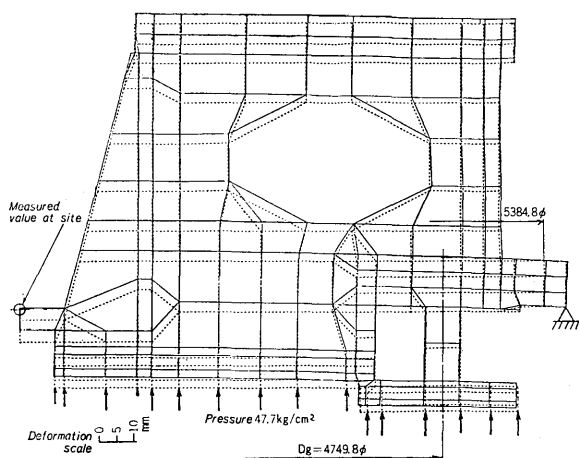


Fig. 12 Comparison of measured values at site and calculated results

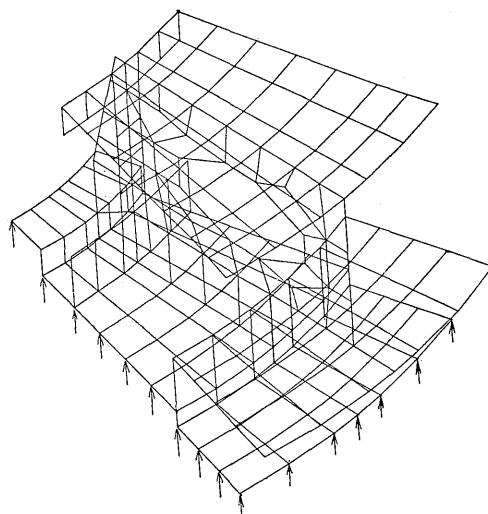


Fig. 13 Input figure of head cover by shell code

cover (refer to Fig. 14) of the recently designed large Kaplan turbine ( $H=22$  m,  $P=59$  MW, runner diameter  $=6,400 \phi$ ) at maximum static head. For the boundary conditions in respect to flange connection parts of the outer and inner head covers, the calculation was made by assuming that both covers were adhered to each other from the bolt pitch circle to the inside of flange of the inner head cover considering the direction of external forces.

In case of the head cover of such a large size Kaplan turbine, the stress level is low because of the low head and it is more important to investigate the deformation than the stress. In this case, the maximum deformation was about 1.3 mm at the upper bearing part of the inner head cover. Considering this deformation the magnetic center of the generator is assembled.

By performing a detailed stress analysis by FEM at the stage of the design, the reliability of the products can be greatly improved.

## VI. WICKET GATE STRESS ANALYSIS

The stress analysis of the wicket gate of a Francis pump-turbine ( $H=103$  m,  $P=52$  MW) at pump shut-

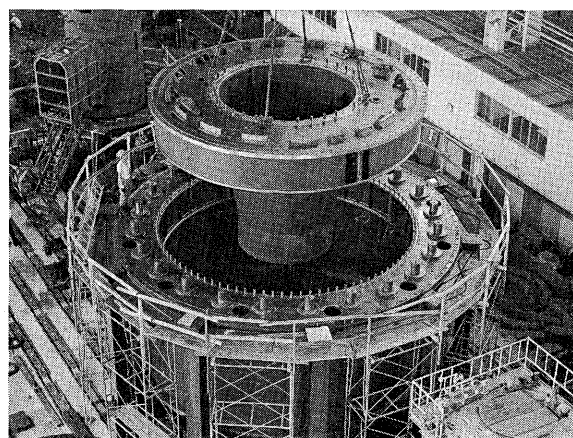


Fig. 14 View of head cover of large Kaplan turbine



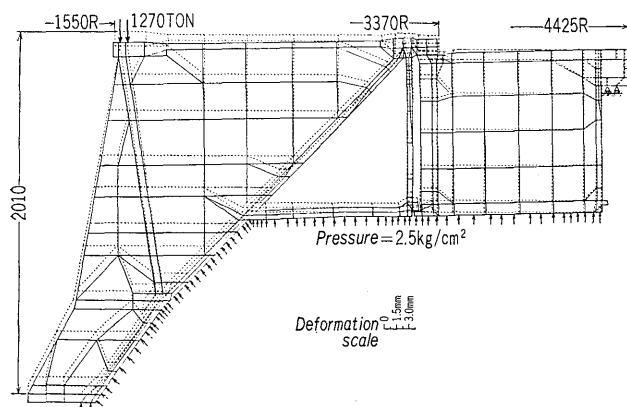


Fig. 15 Deformation figure of head cover of large Kaplan turbine ( $H=22$  m,  $P=59$  MW)

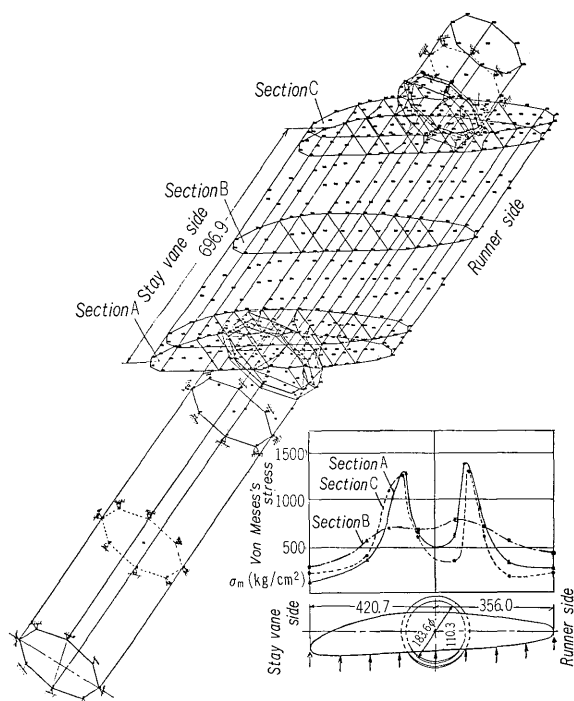


Fig. 16 Wicket gate of Francis pump-turbine ( $H=103$  m,  $P=52$  MW)

off head was performed using the three dimensional solid program. Fig. 16 shows the input figure and the stress distribution by the computation. As the boundary conditions, the shaft end at the head cover side was fixed, the bearing parts were free only in the circumferential direction and the pressure acted on the vane was  $14.5 \text{ kg/cm}^2$ .

The von Mises's formula was used for evaluation of the stress of the solid body. The computed results of this stress distribution are shown in the figure. The stresses in the figure are shown for section A: the end section at the head cover side, section B: the center section of the wicket gate height and section C: the end surface at the discharge ring side. There are large stress concentrations at the junctions between the shaft and vane of the wicket gate.

Such stress concentrations were not found by calculations using the beam theory performed previously.

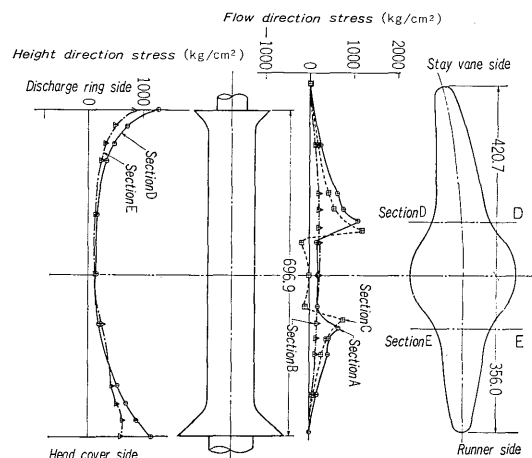


Fig. 17 Modified guide vane with fillet

The locations of the stress concentrations and their values could be determined by means of the FEM three dimensional solid program. Analysis is also possible for these stress concentrations using the shell program. An example is given below.

The analysis was performed with the shell program when fillets were attached to the junction between vane and shaft in order to avoid stress concentrations. As an example Fig. 17 shows the stress distribution in the flow direction and the height direction of the wicket gate. In both stress distributions, there were stress concentrations in the shaft junction parts. However, the values were small and the fillets were effective. The stress concentrations can be reduced by providing such a fillet.

In the wicket gates of high head pump-turbine, the vane height is low so the effective flow area between the wicket gates is reduced when a large fillet is attached to avoid stress concentrations. Therefore, investigations are necessary to find a type of fillet which will minimize the stress concentrations without reducing the effective flow area.

## VII. RUNNER STRESS ANALYSIS

### 1. Pump-Turbine Impeller-Runner

Since the runners rotate in the water and are subjected to large pressure differences, it was very difficult to perform stress analysis by numerical analysis methods. Through the development of the FEM, it has become possible to perform stress analyses

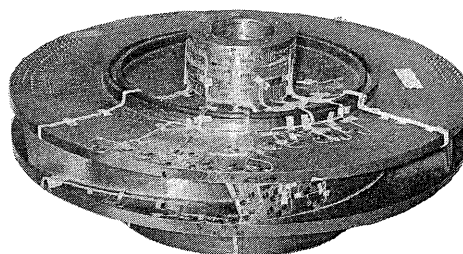


Fig. 18 Model pump-turbine impeller-runner for stress test

even for complex profiles such as those of the Francis runner. The external forces which act on the runners are hydraulic pressure difference and centrifugal force. However, since these pressure difference and the centrifugal force are exerted in the reverse direction at the rated output operation, the stress level is relatively low. Therefore in the case of runner stress analysis, it is necessary to perform the analyses at the runaway speed state with small pressure difference and large centrifugal force and at turbine starting which is the opposite case when only large pressure difference are applied. The stress analysis here was performed in the case of centrifugal force.

A model impeller-runner 640 mm in diameter for the 500 m class pump-turbine was manufactured for stress test. The locations where stress concentrations might occur were obtained by preliminary calculations using the FEM. Based on these results, the stress was measured by attaching strain gauges. Fig. 18 is a photo of the model impeller-runner.

Equipment was used by which the test speed could be changed freely. Since the operating condition for the maximum centrifugal force is the runaway speed state, the test results were converted at the speed equivalent to the actual runaway speed (peripheral speed of 100 m/s). The following relation is established between the stresses of the prototype and model runners:

$$\frac{\sigma_m}{\sigma_p} = \frac{1}{S^2} \cdot \frac{\gamma_m}{\gamma_p} \cdot \frac{n_m^2}{n_p^2}$$

where:  $\sigma$ : stress,  $S$ : dimension ratio of both,  $\gamma$ :

runner specific weight and  $n$ : RPM.

The suffix  $m$  indicates the model and  $p$  the prototype.

The experimental speed was selected so that in the above equation,  $\sigma_m = \sigma_p$ .

Fig. 19 shows the stress figure for the runner calculated by the axisymmetric program. Since the runner vane of the Francis pump-turbine is almost cylindrical, the calculation was made by regarding the cross section of the vane as axisymmetrical when the runner was sectioned radially. The analysis was performed for various case of cross sections but only that showing maximum stress is indicated in the figure. A comparison is shown with the measured results for the stress distributions on the upper surface of the crown and the surface of the vane. The broken lines show the measured values and the solid lines the computed values.

It is evident from this figure that there is also sufficient agreement with the analysis when considering it as axisymmetrical. The runner vane is bent by the deflection of the runner band. Therefore the stress on suction surface (inside surface) of vane is compressive on the band side and tensile on the crown side. This also influences the stress distribution of the crown. Therefore compressive stress appears on the upper surface of the crown near the vane inlet at the inside junction of the vane and crown.

The stress calculation of the runner vanes were executed formerly by means of the beam theory assuming both ends fixed (Fig. 20 (a)). However, in

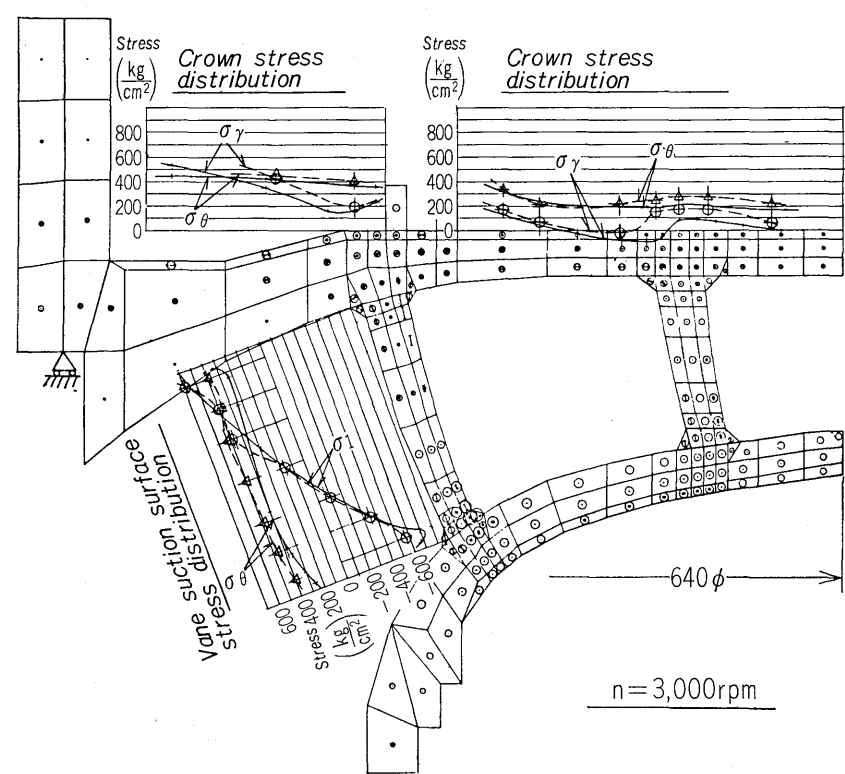


Fig. 19 Stress figure of pump-turbine impeller-runner

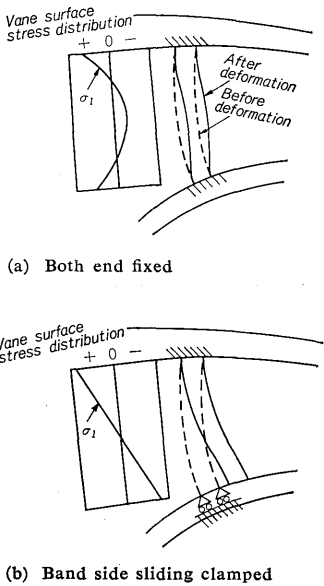


Fig. 20 Boundary condition of runner vane

practice, the stress mode is similar to that of the beam theory assuming a sliding clamp on the vane band side (Fig. 20. (b)).

In order to investigate the stress distribution in the circumferential direction on the crown, the deformations obtained by the axisymmetric program was used as input and the analysis was made using the shell program. The results are shown in Fig. 21. In this analysis, a cyclic segment which is subjected to the great influence of the bending due to the vane

was picked out. There was almost no influence of the bending near the outer periphery of the crown (section B-B) because of the free end and the stress distribution of the crown was almost uniform in the circumferential direction. However, the influence of the bending is appeared near the center of the crown (section C-C) and the stress distribution was cyclic from the center of a vane to the center of the next vane. This stress distribution can also be obtained with sufficiently high accuracy using the shell program.

## 2. Split Runner for Pump-Turbine

In accordance with the larger capacity tendency of pumped storage hydroplants, there are many cases of hydro-turbine runners being splitted because of transport limitations.

A model split runner 466 mm in diameter was manufactured, strain gauges were glued to the flange bolts and the stress of the bolts due to centrifugal force was obtained. The stress on the crown and vane surface was measured simultaneously. The experimental equipment is shown in Fig. 22.

Fig. 23 shows the stress figure analyzed by the same method as in clause 1. The measured values in the figure are shown by the symbols  $\triangle$  and  $\oplus$ . There is good agreement with the computed values of the stress distribution for both the crown and vane surface.

Moreover in order to investigate stress imposed on the bolts, an analysis was performed on one half of the crown divided into two parts using the plane program. The results are shown in Fig. 24. Since the force exerted is only the centrifugal forces, the analysis was performed by concentrating the total forces at the center of gravity of the divided crown. The computed values are almost the same as the measured values of the forces applied to the various bolts. From this analysis, it is evident that the force exerted on the bolts becomes larger as the radius of rotation becomes smaller and in the design, it is desirable that the diameter of the bolts is increased as the radius of rotation becomes smaller.

## VIII. CONCLUSION

The stress analysis by FEM of hydro-turbine components was explained by the above examples. However, the FEM code is only a design tool although it is very powerful. Therefore, even if a part of safety factor should be improved because of incorrect stress calculation in the past, the permissible stress should also be considered from the standpoint of reliability in respect to the material characteristics (especially fatigue strength in water) and the production methods, inspection techniques. There should not also naturally be abrupt changes in the design concepts in accordance with the development of the FEM code.

However, if the highly sophisticated utility tech-

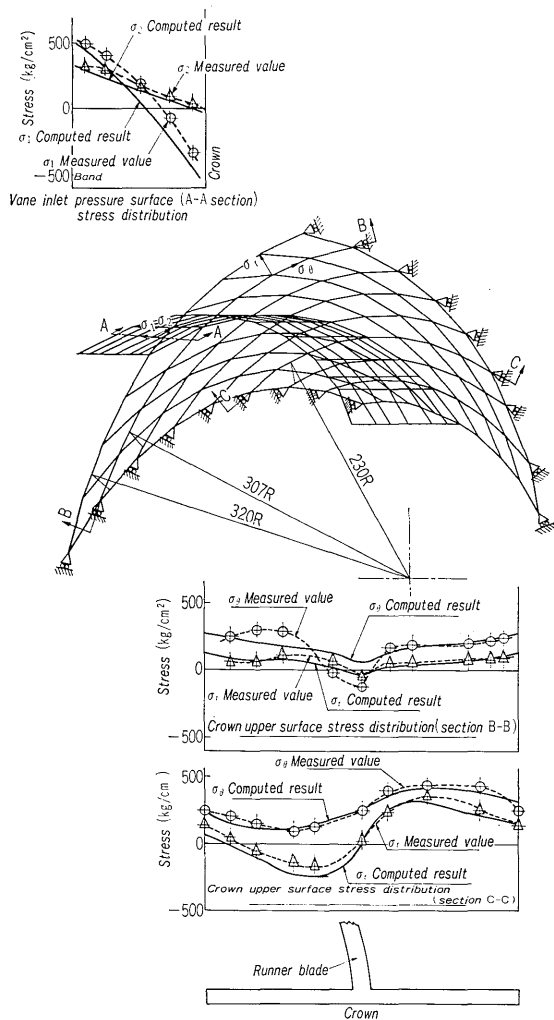


Fig. 21 Stress distributions of runner crown by shell analysis

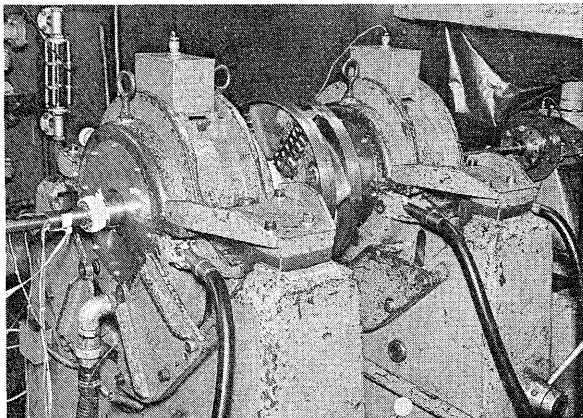


Fig. 22 Model split runner under stress test

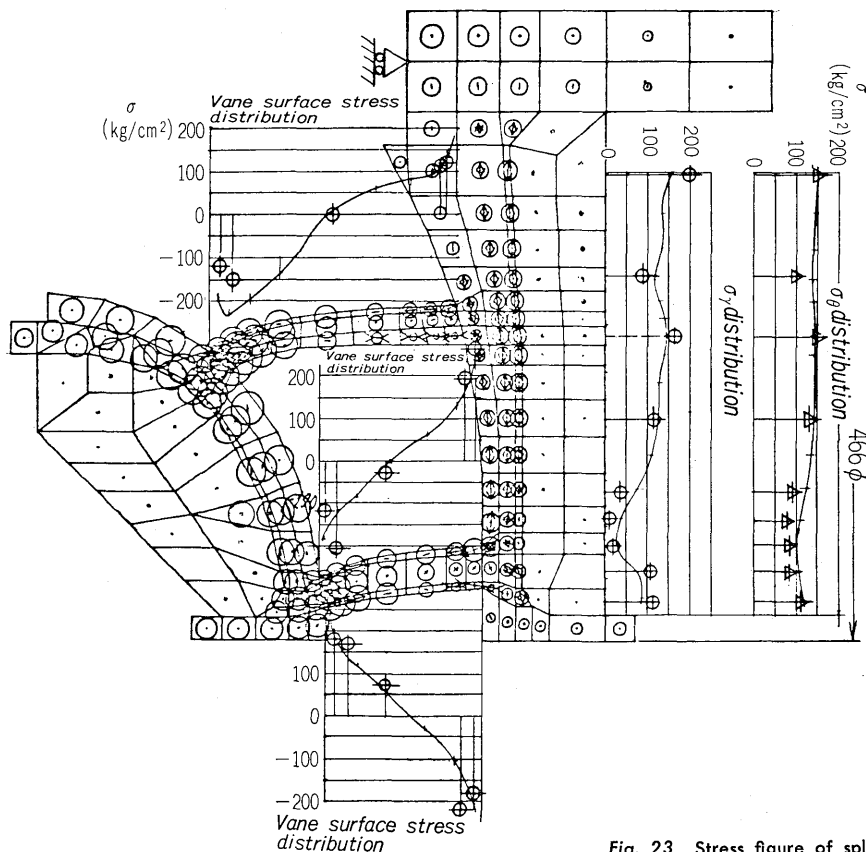


Fig. 23 Stress figure of split runner

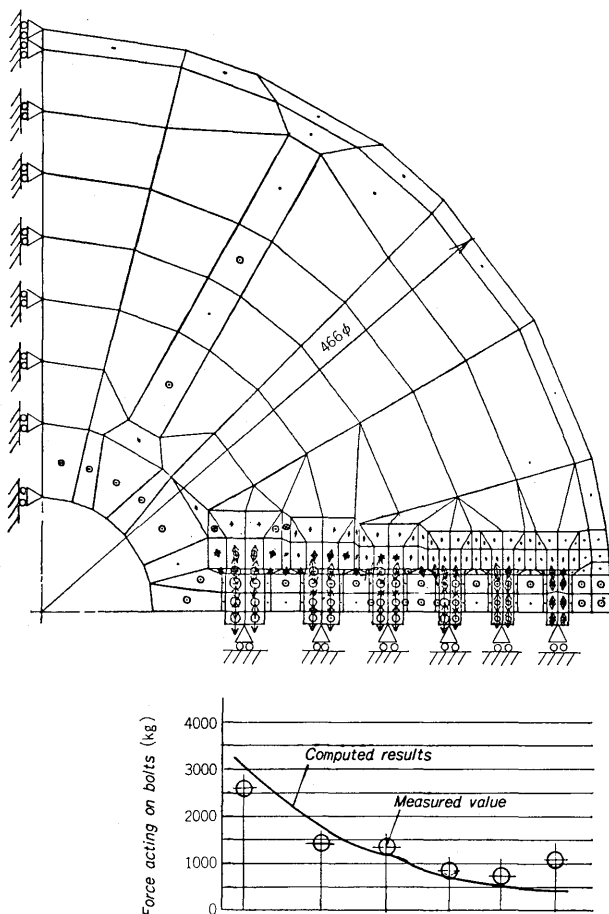


Fig. 24 Stress figure of flange parts of split runner

niques are established, stress concentrations and deformations in complex structures will be able to be detected by the FEM with greater accuracy and this will be of great importance for the large capacity, high head and high speed tendency of hydro-turbine and pump-turbine. It will be of great value to be able to perform stress analysis easily for the various design conditions at the projection and structural design stages so that the most suitable structure with smaller deflection and stress concentrations can be selected.

This article was limited to the static stress analysis of hydro-turbine components but there has recently been remarkable progress in the application of the FEM to dynamic response and it is hoped to present an article concerning the dynamic response of hydro-turbine components in the near future.

## References

- (1) C.A. Felippa, "Refined Finite Element Analysis of Linear and Nonlinear Two-dimensional Structures", SEL Report No. 66-22, University of California, Berkeley (1966)
- (2) R.W. Clough and J.L. Tocher, "Finite Element Stiffness Matrices for the Analysis of Plate Bending", Proceedings of the Conference on Matrix Methods in Structural Mechanics, AFIT, Ohio (1965)
- (3) J.H. Argyris and D.W. Scharpf, "The Curved Tetrahedral and Triangular Elements TEC and TRIC for the Matrix Displacement Method", The Aeronautical Journal of the Royal Aeronautical Society, Jan (1969), pp. 55~65.
- (4) "Determine Stresses in Metal Spiral Case for Hydraulic Turbines" NEMA PUB NO. HT3-1957
- (5) J. Parmakian, "Stresses in a Hydraulic Turbine Stay Ring", Trans. of the ASME Paper No. 62-WA-166